A wide range of applications such as healthcare, human comfort, agriculture, food processing and storage, and electronics manufacturing also require fast and accurate measurement of humidity and temperature. Optical fiber-based sensors have several advantages over electronic sensors, and much research has been conducted in this area in recent years. This paper describes the current trends in fiber optic temperature and humidity sensors. The evolution of optical structures aimed at humidity detection is presented, as well as a new design of an optical sensor used for this purpose.

The main methods of humidity determination using fiber-optic laser reflection based on Optical fiber humidity sensor (FPI) were analyzed and experimental results were obtained. Based on temperature-sensitive strain variation, a method for temperature determination based on the specific spectral back-reflection effect of fiber Bragg gratings (FBGs) is considered. Experimental analyses were conducted on the light reflection of humidity-sensitive agarose using optical fibers based on the Fabry-Perot Interferometer (FPI). It exhibits a good linear response to relative humidity, ranging from 25 % to 95 %. During temperature measurement, the deformation changes of the Fiber Bragg Grating fibers showed excellent performance, ranging from –5 °C to 70 °C.

New structures, such as resonators, are being explored to improve the resolution of fiber optic temperature and humidity sensors. In addition, recent studies on polymer optical fibers show that the sensitivity of this type of sensor has not yet been achieved. Thus, materials sensitive to humidity and temperature still need to be investigated to improve sensitivity and resolution

Keywords: Fabry-Perot interferometer, fiber Bragg Grating, relative humidity, optical fibers

UDC 53.087.92
DOI: 10.15587/1729-4061.2024.306711

IMPROVEMENT OF FIBER OPTIC SENSOR MEASUREMENT METHODS FOR TEMPERATURE AND HUMIDITY MEASUREMENT IN MICROELECTRONIC CIRCUITS

Anar Khabay
Corresponding author
Doctor PhD, Associate Professor*
E-mail: a.khabay@satbayev.university
Murat Baktybayev
Candidate of Physical and Mathematical Sciences, Associate Professor
Department of Robotics and Technical Means of Automation**
Serikbek Ibekeyev
Master of Technical Sciences, Senior Lecturer*
Nurlan Sarsenbayev
Candidate of Technical Sciences, Associate Professor
Department of Automation and Control**
Nuridin Junussov
Senior Lecturer*
Nurzhan Zhumakhan
Senior Lecturer, Master of Technical Sciences, Lecturer
Department of Automation and Robotics
Almaty Technological University
Tole bi str., 100, Almaty, Republic of Kazakhstan, 050012
*Department of Electronics, Telecommunications and Space Technologies**
**Satbayev University
Satbayev str., 22, Almaty, Republic of Kazakhstan, 050013

Received date 08.04.2024
Accepted date 13.06.2024
Published date 28.06.2024

***How to Cite**: Khabay, A., Baktybayev, M., Ibekeyev, S., Sarsenbayev, N., Junussov, N., Zhumakhan, N. (2024). Improvement of fiber optic sensor measurement methods for temperature and humidity measurement in microelectronic circuits. Eastern-European Journal of Enterprise Technologies, 3 (7 (129)), 36–44. https://doi.org/10.15587/1729-4061.2024.306711*

1. Introduction

In modern society, the role of temperature and humidity measurement technologies is critically important. Technological progress, environmental changes, and new requirements in healthcare systems necessitate constant monitoring of these parameters. Consequently, the development of sensors based on optical fibers remains highly relevant, as this technology is widely used in industrial applications, scientific research, and medical devices.

Despite research underscoring the significance of this topic, many issues remain unresolved. For instance, ensuring high sensitivity and reliability in measuring temperature and humidity with sensors is still a pressing issue. This, in turn, necessitates further research and technological advancements.

Optical fiber sensors offer numerous advantages when implemented in microchips, enhancing the efficiency and functionality of electronic devices. These sensors are resistant to electromagnetic effects, making them highly suitable for use in environments with electromagnetic noise, particularly in medical devices and industrial automation. The micro-size of optical fibers facilitates their installation in microchips, reducing the overall size of the devices and enhancing their mobility. Many optical fibers possess chemical stability, which allows for highly accurate measurement of chemical concentrations even in harsh environments.

Various types of fiber optic sensors have been proposed for detecting humidity based on crystalline fibers [1–3]. Applications of optical fibers in temperature measurement methods have been demonstrated [4]. Sensitivities based on optical fiber Bragg gratings [5–7] and Fabry-Perot interferometers [8, 9], as well as single-mode optical fibers [10], have been discussed in publications. The use of agarose gel, which has low consumption, easy preparation, and good results in calculations, is often employed for comparative humidity [11]. To enhance the sensitivity of optical fibers, they are made from hygroscopic materials such as agarose gel, graphene oxide, polyvinyl alcohol, silicon dioxide (SiO_2), Tungsten disulfide (WS_2), and others. In recent years, sensors based on the intrinsic sensitivity of optical fiber lasers have been extensively studied because they can improve the visibility of the spectral resonance peak and reach a 3-dB transmission capability [12].

By developing proprietary sensing based on fiber lasers, we improved the signal-to-noise ratio of the sensors and increased the capacity of the sensor network based on 3 dB narrowband transmission. This paper, based on fiber optic FPIs (Fabry-Perot interferometers) obtained experimental results in the range of humidity from 25% to 95% and analyzed based on FBGs deformation the possibility of temperature determination by the back reflection spectrum.

2. Literature review and problem statement

Fiber optic sensors are widely used in temperature and humidity monitoring studies due to their simple design, low cost, fast response time, high sensitivity, and unique intrinsic safety advantages. In [13], these characteristics are discussed in detail with a focus on practical applications of fiber optic sensors in various environments. However, the study did not consider the long-term stability of the sensors under fluctuating environmental conditions, which remains a critical issue for continuous monitoring applications.

In [14], it is emphasized that fiber optic sensors are immune to electromagnetic interference, which makes them ideal for use in environments with high levels of electromagnetic noise, such as industrial facilities and medical facilities. However, this study did not consider the possibility of mechanical vibration affecting the accuracy of the sensors, which can be a serious problem in environments with heavy machinery or moving parts.

Fiber optic surface plasmon resonance (SPR) sensors are characterized by high sensitivity and structural diversity, as discussed in [15, 16]. These studies have demonstrated the potential of SPR sensors in detecting minute changes in environmental parameters. Despite these advantages, the studies did not investigate the long-term effects of environmental pollutants on sensor performance, which is very important to ensure reliable performance over a long period of time.

However, in transmission and power spectrum measurements, measurement errors occur due to interference from temperature and humidity, which can affect the accuracy of the sensors. In [17, 18], a new method for fabricating an interferometric Fabry-Perot sensor was proposed. In these studies, photopolymerizable materials were used to create Fabry-Perot interference structures, which solved some measurement problems. However, this method requires a complex structure for simultaneous measurement of two parameters, resulting in increased cost and difficulty in fabrication.

In [19] and [20], a new type of two-parameter salinity and temperature sensor based on a fiber ring laser (FRL) with a side-hole fiber (SHF) embedded in a Sanyak interferometer is presented. Although this approach offers innovative solutions, it still suffers from drawbacks such as low sensitivity and difficulties in fabrication technology. These studies did not consider potential improvements in fabrication techniques that could improve the sensitivity and reliability of the sensor, indicating a gap in current research.

Although the simultaneous measurement of temperature and humidity based on fiber Bragg grating (FBR) has excellent linearity and stability, as noted in [21] and [22], the process of eliminating the mutual influence of the parameters while maintaining the same sensitivity to both physical quantities is complex. This complexity presents a major challenge for practical implementation. The cited studies did not present a clear methodology to simplify this process, which is necessary for wider application and adoption of FBR-based sensors.

In [23], recent advances in single and multi-parameter sensing and measurement of TSP (temperature, salinity, pressure) using various fiber optic sensors (FOS) are reviewed. However, despite the detailed analysis, the study did not propose specific solutions for achieving stable fabrication quality or adapting sensors to rapidly changing conditions, which leaves considerable room for further research and development.

Accurate measurement of two parameters simultaneously using a Fabry-Perot interferometer requires a complex structure. This increases manufacturing costs and limits the sensor options.

Based on Fiber Bragg Grating (FBR), it is difficult to eliminate the mutual influence of parameters when measuring temperature and humidity simultaneously. This may reduce the measurement accuracy. Therefore, to solve this problem, a new structure or algorithms are needed to eliminate the influence of parameters.

Some studies have not considered the long-term stability of fiber optic sensors. The stability problem is related to factors such as environmental factors, material aging, and design degradation. Long-term testing and research are needed to solve this problem.

3. The aim and the objectives of the study

The aim of this study is to develop a new sensor with a simple structure, in which the measurement parameters based on microstructured optical fiber do not affect each other, and to develop approaches that ensure its long-term stability. This will make it possible to provide reliable and continuous monitoring of temperature and humidity in industrial and medical environments by developing a new sensor device. With this device, it is envisaged to improve the efficiency of monitoring systems by introducing highly accurate and electromagnetic interference resistant sensor systems in industrial processes and medical facilities.

To achieve this aim, the following objectives are accomplished:

– to investigate behavior the effectiveness of measurement parameters using a combination of Fabry-Perot interferometer and Fiber Bragg Grating to improve the ability to accurately measure temperature and humidity;

– to determine the sensor response time as a function of environment and the variation of sensor parameters as a function of temperature;

– to check the influence of external factors, mechanical vibrations on the accuracy of the sensor.

4. Materials and methods

Let's analyze methods for measuring temperature and humidity based on the structure of a novel sensor based on microstructure optical fiber. The operating principle of the proposed sensor is based on two main sensitivity parameters. determination of relative humidity of the environment based on the surface reflection of the moisture-sensitive agrozine gel using a Fabry-Perot interferometer. Temperature determination using fiber Bragg gratings (TBTs) based on the temperature-dependent fiber strain change.

Temperature monitoring is carried out as shown in Fig. 1 using an optical fiber Bragg grating that is coated with acrylate and sensitive to temperature. Spectrum reverses reflection effect of the optical Fiber Bragg Grating.

It is called the Bragg wavelength (λ_B), and located in the middle of the waves which is the lumen of the filter to achieve the light spectrum that can satisfy the requirements of Bragg [24].

The value (λ_B) of these gratings in most sensing temperature applications can be expressed as:

$$\lambda_B = 2\cdot\Lambda\cdot\eta_{eff}. \quad (1)$$

In practice, the effective refractive index of the core and the spatial periodicity of the grating are both affected by changes in strain and temperature. In particular, the effective refractive index is modified through the thermo-optic and strain-optic effects, respectively. Hence, from (1), the Bragg wavelength shift $\Delta\lambda_B$ due to strain $\Delta\varepsilon$ and temperature ΔT variations is given by [25]:

$$\Delta\lambda_B = 2\left(\Lambda\frac{d\eta_{eff}}{dT}+\eta_{eff}\frac{d\Lambda}{dT}\right)\Delta T + \\ +2\left(\Delta\frac{d\eta_{eff}}{d\varepsilon}+\eta_{eff}\frac{d\Lambda}{d\varepsilon}\right)\Delta\varepsilon. \quad (2)$$

The first term in (2) represents the effect of temperature on the Bragg wavelength. The Bragg wavelength shift due to thermal expansion comes from the modification of the grating spacing and the refractive index. The relative wavelength shift due to a temperature change ΔT can be written as:

$$\frac{\Delta\lambda_B}{\Delta T}=\lambda_B\left(\frac{1}{n_{eff}}\frac{dn_{eff}}{dT}+\frac{1d\Lambda}{\Lambda dT}\right), \quad (3)$$

where $\frac{1}{n_{eff}}\frac{dn_{eff}}{dT}$ is the thermo-optic coefficient, which is approximately equal to 8.6×10^{-6} K^{-1} for germanium doped silica core optical fiber and $\frac{1d\Lambda}{\Lambda dT}$ is the thermal expansion coefficient of the optical fiber, which is approximately equal to $0.55\times10^{-6}K^{-1}$ for silica so that the refractive index change is by far the dominant effect [26]. The order of magnitude of the temperature sensitivity of the Bragg wavelength is 10 pm/°C around 1,550 nm. Λ is the spatial period of the Bragg grating, and n_{eff} is the effective reverse refractive index of the optical single mode fiber. These two parameters are the function of strain and temperature. Optical Fiber Bragg Grating sensors (sensors shown in Fig. 2) are popular for detecting temperature strains [27]. The Bragg wavelength shift ($\Delta\lambda_B$) induced by either a strain(ε) or temperature change (ΔT) is expressed by the following equation:

$$\frac{\Delta\lambda_B}{\lambda_B}=(1-P_e)\varepsilon+[(1-P_e)a+\xi]\Delta T, \quad (4)$$

where respectively, P_e is the photoelastic constant, α is the thermal expansion coefficient, and ξ is the thermo optic coefficient of the optical single mode fiber.

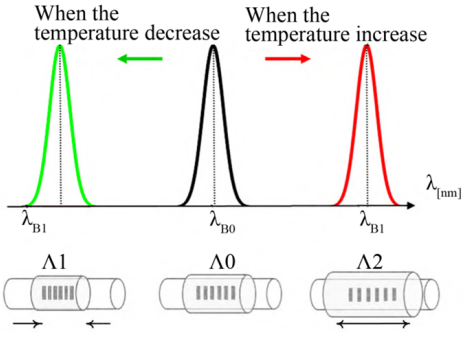

Fig. 1. The image shows the lengths and the spatial periods of the gratings as well as the Bragg wavelengths at three different temperature values

Based on the Fabry-Perot, an interferometer is sensitive to humidity. The scheme of the humidity-sensitive FPI diagram is shown in Fig. 2, *a*. As shown in Fig. 2, *b*, a single-mode optical fiber with a Bragg Grating is installed and its transverse cross-section is connected to the FPI vacuum cavity, which is covered with a moisture-sensitive film. A silicone diaphragm covers the vacuum cavity of the FPI. In Fig. 2, *a* the silicon diaphragm deposited with Agarose. There are two reflective surfaces which are front and back of the vacuum cavity, whose length is defined as *h*. Due to occurrence of interference between these two surfaces, light reflects. Because of the thickness of the silicon diaphragm on the Agarose gel, both are much less than the length of the vacuum cavity. Agarose gel has been seen as one reflective surface in the theoretical model. Therefore, the total reflected electric fields E_r of the FPI [28]. The FPI can have the reflected electric field of two pages as follows:

$$E_r = E_0\left[\sqrt{R_1}+(1-a)(1-R_1)\right], \quad (5)$$

where E_0 is the input electric field, α is the transmission loss factors. R_1 and R_2 are the reflection coefficients of the two reflective surfaces. φ_{FRI} is the round-trip propagation phase shift, which can be given by:

$$\varphi_{FRI}=\frac{4\pi h}{\lambda^{\circ}}. \quad (6)$$

Therefore, the peak wavelength of the m-th order is given by:

$$\lambda_m=\frac{2h}{m}, \quad (7)$$

where m is an integer. It is possible to derive the free spectral range, and the wavelength spacing between the two adjacent dips can be expressed as:

$$\Delta\lambda_m = \frac{\lambda^2}{2h}. \quad (8)$$

Total reflection spectra $I(\lambda)$ of the FPI is sensitive to humidity can be described as:

$$f(\lambda) = \left|\frac{E_r}{E_0}\right|^2 = A + B\cos(2\varphi_{FR}), \quad (9)$$

where:

$$A = R_1 + (1+a)^2 (1+R_1)^2 R_2,$$

$$B = \sqrt{R_1 R_2}(1-a)(1-R_1). \quad (10)$$

According to Frenel formula, the reflection coefficient of the agarose gel can be written as:

$$R_2 = \left(\frac{n_A - 1}{n_A + 1}\right)^2, \quad (11)$$

where n_A is the refractive index of the Agarose. When the refractive index of Agarose changes, the reflectance at the second surface will change. Because the refractive index of agarose is sensitive to ambient humidity. FPI can used to determine the humidity content of the wavelength I(λ) below:

$$f(\lambda) = R_1 + (1-a)^2 (1-R_1)^2 \left(\frac{H_\varepsilon A - 1}{H_\varepsilon A + 1}\right)^2 +$$

$$+2\sqrt{R_1}(1-a)(1-R_1)\left(\frac{H_\varepsilon A - 1}{H_\varepsilon A + 1}\right)\cos(2\varphi_{FR}). \quad (12)$$

As it is analyzed above, the working principle of the proposed sensor is based on two main sensitivities. Firstly, humidity-sensitive agricultural reflection based on the Fabry-Perot interferometer method; secondly, the phase change in fiber deformation dependent on temperature changes based on the specific spectra back-reflection effect of Optical Fiber Bragg Gratings (OFBG). With special attention to the efficiency and accuracy of the sensor, let's conduct experimental tests on the new design of optical fiber sensors designed for simultaneous measurement of temperature and humidity to evaluate the response speed and sensitivity of the sensor during functionality testing.

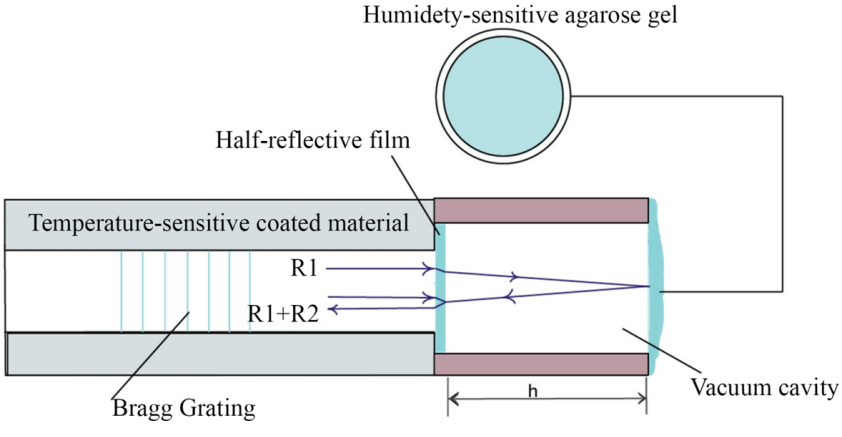

a

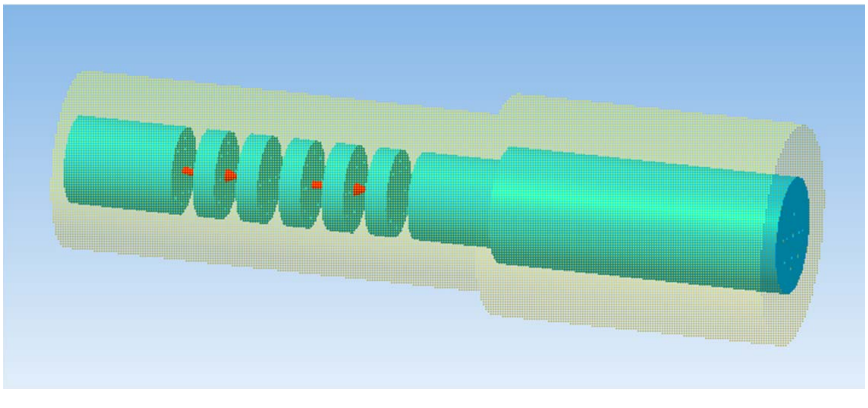

b

Fig. 2. Schematic of the principle of operation of the sensor based on two main sensitivities:
a — 2D view of a fiber-optic sensor;
b — 3D view of a fiber-optic sensor

5. Results of development of leach algorithm optimization

5. 1. Investigation of the efficiency of measurement of sensor parameters

Performing expert analysis of PCI-based relative humidity determination using moisture-sensitive composite fiber based on surface modification of agarose gel [29].

Fig. 3 presents the general schematic of the experimental setup for testing the closed sensor. The experimental setup of the sensitive humidity based on FPI defines the fiber Bragg grating sensitivity that depends on the temperature. The spectrum wavelength from the optical fibrous source of the laser is 1500 nm. The gain medium of the fiber laser is the Erbium-doped fiber with a length of 3 meters. In the fiber ring cavity, there is an isolator, which controls unidirectional flow. The sensors are inserted in the fiber laser by a circulator and the transmission optical fiber (TOF, Thorlabs). The vacuum cavity of FPI serves as a wavelength-selective filter and is used as the sensing head for humidity detection. Optical spectrum analyzer (OSA, YOKOGAWA, AQ6370, spectral resolution 0.02 nm) connects the three-output spectrum. There are two spectrum values alternately analyzed, where first spectrum reverses reflection effect of the optical Fiber Bragg Grating and second when the ambient humidity of the sensing head changes the power reflection of the FPI.

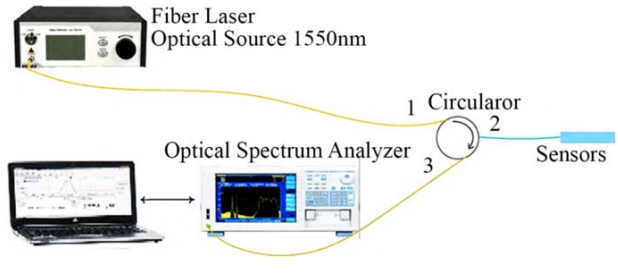

Fig. 3. Experimental setup

In the fabrication of the Fabry-Perot interferometer, the production of the silicon diaphragm employs mature micro-electromechanical system fabrication techniques, which provide capability of batch-production and we have reported that in [30]. The thickness of the silicon diaphragm is about 10 μm with dimension 2.5 mm×2.5 mm. The two reflecting surfaces are at the center in a vacuum environment. Then, the 2 % Agarose gel deposited on the silicon diaphragm by a pipette. Agarose gel is prepared by dissolving the agarose powder in distilled water in the beaker. In the deposition process, the thickness of the Agarose is about 1μm.

In order to obtain the optimized SNR of the proposed humidity sensor, the sensor fabrication should ensure the spectral overlap between the peak in the spectrum of the FPI. In the experiments, the gain peak at about 1500 nm is selected for the intracavity sensing. The peak wavelength and the wavelength spacing of the FPI can be designed by changing the h length of the FP cavity. When the ambient humidity is 35 %RH, the reflection spectrum of the FPI is measured as in Fig. 4. In the reflection spectrum of the Fabry-Perot interferometer, the peak with maximum intensity is at about 1530 nm and the reflection loss is –12.2 dB. The wavelength of the FPI is 15.5 nm.

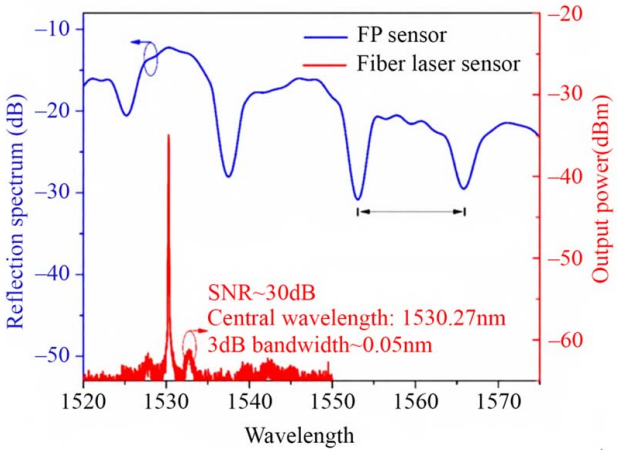

Fig. 4. The spectra of the Fabry-Perot interferometers and corresponding optical fiber when the ambient relative humidity is 35 %

Based on the FPI method, the relative humidity range is 20–98 % RH. As the ambient humidity changes, the output spectra of the optical fiber laser are measured as shown in Fig. 5. The output power of the optical fiber laser increases from – 36.78 dBm to – 22.61 dBm as the ambient humidity changes from 25 %RH to 95 %RH with the resolution of 10 %RH. Accordingly, the signal-to-noise ratio increased from 30 dB to 45 dB and the transmittance was 3dB, which was lower by 0.5nm. The humidity sensitivity is measured to be 0.202 dB/ %RH. It shows the sensor has a good linear response. The practice showed a good outline of the sensor. So, as the relative humidity of the environment has changed from 20 % to 90 %, The agglomerate breakdown index is measured from 1.45 to 1.48.

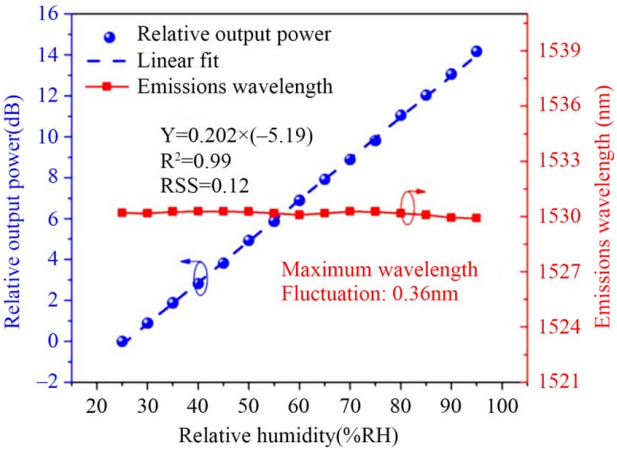

Fig. 5. The change in the optical fiber laser output spectrum when the ambient humidity varies from 20 % RH to 90 %RH

The sensitivity of the sensor to relative humidity is from 20 % to 98 % based on the Fabry-Perot interferometer. Experimental results show that it has a linear response, that is, its response is determined by the refractive index of Agrose, which is directly related to the humidity level. Due to this, it is possible to verify that the sensor works reliably.

5. 2. Determination of the sensor response time depending on the environment

Microstructured optical fiber sensors occupy an important place in modern monitoring systems. These sensors enable accurate measurement of ambient temperature and humidity and are widely used in various industrial and research applications. In this study, the response and reset times of the sensor as well as the sensitivity characteristics related to temperature changes were analyzed.

In Fig. 6, *a*, the sensor's approximate response time reaches 72 ms, while the recovery time is about 357 ms, which relates to the moisture output from the sensor depending on the air time. Considering the insertion and removal time, the actual response time and recovery time will be shorter than the measurement time. This indicates the sensor's quick response capability.

In Fig. 6, *b*, cross-sensitivity of the sensor is the laser spectrum of the fiber at any temperature. As the temperature increases from 25 °C to 45 °C, the release wavelength of the optical fiber laser sensor has a red shift from 1530.19 nm to 1530.64 nm and the output power decreases from – 36.64 dBm to – 37.12 dBm. A low-temperature cross-sensitivity is received as – 0.025 dB/°C and 0.024 nm/°C.

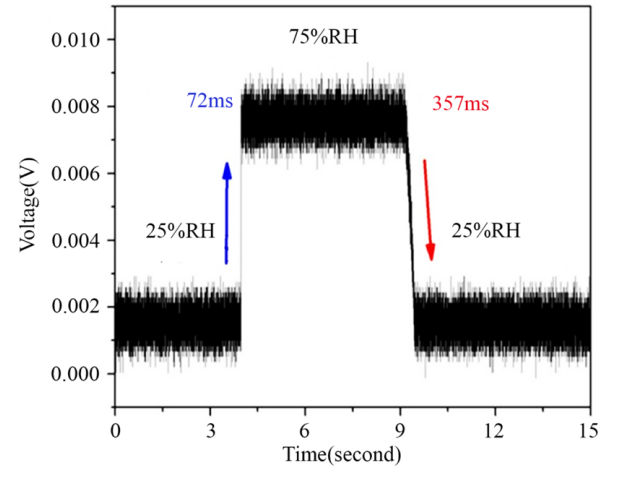

a

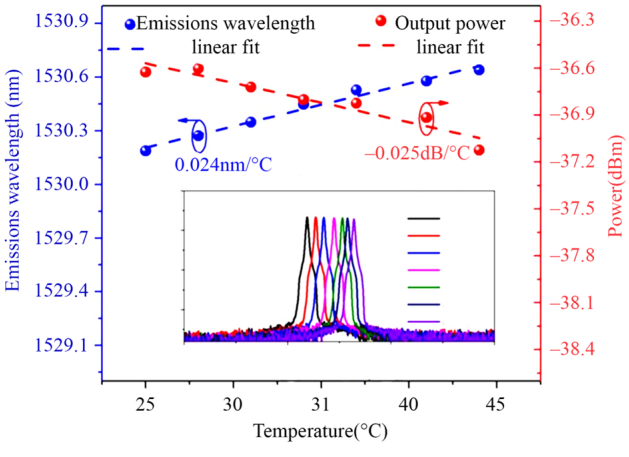

b

Fig. 6. The result obtained to determine the effectiveness and accuracy of the sensor: *a* time-dependent sensitivity response of the sensor; *b* a low-temperature cross-sensitivity is received as – 0.025 dB/°C and 0.024 nm/°C

Study temperature detection using Fiber Bragg meshes based on composite materials for temperature detection applications reported in the literature [31, 32]. The wavelength shift due to temperature change ΔT is defined as $\Delta\lambda$. This is our temperature-sensitive parameter:

$$\Delta\lambda=\lambda_0\times(C_m\times\Delta T), \quad (13)$$

where $\Delta\lambda$ represents the shift in the Bragg wavelength (1550 nm) at a specific temperature. St is the temperature sensitivity coefficient of the FBG (0.01 nm/°C). Based on the Fiber Bragg Grating (FBG), the sensitivity coefficient to temperature changes from –5 °C to 70 °C is listed in the Table 1.

Table 1

The change of the sensitivity coefficient Δλ to temperature change from –5 °C to 70 °C is shown

Temperature (°C)	Wavelength Shift (Δλ, *nm*)
–5	–0.075
0	0.000
10	0.100
20	0.200
30	0.300
40	0.400
50	0.500
60	0.600
70	0.700

According to this table, the wavelength shift changes linearly with temperature from –5 °C to 70 °C. For every 10 °C, the wavelength changes by about 0.1 nm. The sensitivity coefficient of a fiber Bragg grating (FBR) indicates the wavelength shift over a certain temperature range. This shift is temperature dependent. The temperature sensitivity coefficient of the FBR (*St*) is 0.024 nm/°C.

5. 3. Checking the influence of external factors on the accuracy of the sensor

Output stability is an important parameter for internal fiber laser sensors, which limits their applications [32, 33]. For the stability analysis of the fiber sensor, the emission wavelength and output power have been measured over 180 minutes, with the humidity fixed at 65 % RH and 95 % RH, respectively. The optical fiber laser output spectrum is shown respectively in Fig. 7, *a*, *b*. Wavelength and power stability are analyzed in Fig. 7, *c*. The standard deviations of wavelength and power fluctuations are 0.101 nm and 0.129 dBm, respectively, at 65 % RH, and 0.046 nm and 0.137 dBm, respectively, at 95 % RH. This demonstrates that the sensor exhibits good repeatability in its humidity response, and the fluctuation of the measured humidity value is less than ±2 percentage RH.

The new sensor design has been researched and refined to accurately and reliably measure humidity and temperature. It is possible to see the high sensitivity of this sensor and its ability to respond quickly in various environmental conditions. They are also characterized by their ability to resist electromagnetic interference and simple structure. The long-term stability of the sensor is studied only in laboratory conditions.

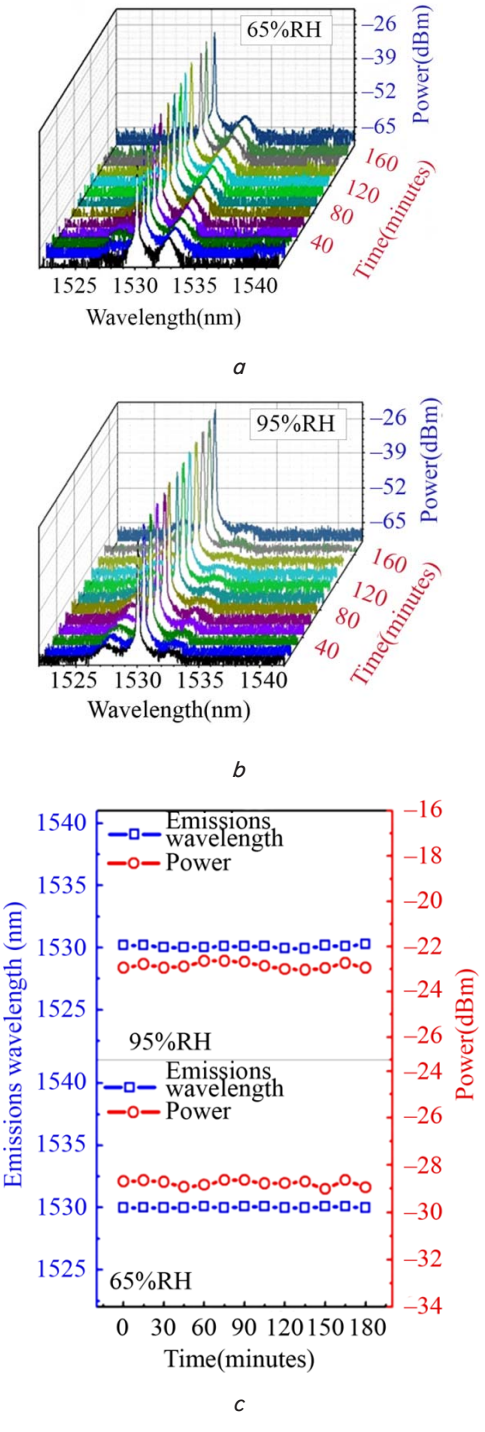

Fig. 7. Fiber optic sensor output spectrum for ambient relative humidity determination: *a* — optical fiber laser output spectrum measured with the humidity fixed at 65 % RH; *b* — optical fiber laser output spectrum measured with the humidity fixed at 95 % RH; *c* — wavelength and power stability

6. Discussion of the results of the sensor research under different operating conditions

Depending on temperature and humidity, the functional materials are mainly composites and synthetics, which are expensive or not degradable. In addition, the production of sensitized composites is usually accompanied by the generation of by-products that cause environmental pollution [34]. Alternatives to natural sensitization are necessary to realize biocompatibility so that implanted sensors are environmentally friendly.

One of the main limitations to the widespread use of such sensors is the cost of expansion and the complexity of maintenance. To reduce costs, mass production of sensor parts is required, as well as simple construction in durable materials to minimize the need for regular maintenance. Moisture-sensitive materials can reduce data reliability due to exposure to dust or contaminants. Therefore, they required protective membranes or additional components. Accordingly, thin functional coatings or thin optical fibers tend to respond faster and have higher sensitivity [35]. Thick coatings cannot provide high sensitivity. This requires additional optimization in parameter selection.

The structure of the discussed fiber-optic sensors is designed, which mainly consists of two independent parts: the first is a vacuum Fabry-Perot interferometer (Fig. 1, *a*) with a moisture-sensitive agarose gel absorption indicator, and the second is light filters located in the middle of the optical fiber that satisfy the condition of temperature-sensitive Bragg gratings (Fig. 1, *b*).

In (2), (3), the effect of Bragg wavelength on temperature is described. Moisture determination based on the Fabry-Perot interferometer method is described by the reflection coefficient of the Agarose gel using the Fresnel formula as in equation (11). where *nA* – when the refractive index of agarose changes, the reflection from another surface changes. Since the refractive index of agarose is sensitive to the humidity of the medium I(λ), let us formulate equation (12) to determine the humidity as a function of wavelength. The experiments were conducted based on these analyses.

Experiments have used a light wavelength of approximately 1500 nm. The relative humidity based on the FPI method ranges from 20 % to 98 %. When the ambient humidity changes, the output spectrum of the fiber laser, as shown in Fig. 5, indicates that the output power of the fiber laser increases from –36.78 dBm to –22.61 dBm. The experimental results demonstrate the sensor's linear response to humidity. As shown in Fig. 4, the estimated response time of the sensor was 72 ms. The recovery time was about 357 ms, which is due to the moisture retention in the air. Considering the exposure and elimination times, it is possible to assume that the actual activation and recovery times are shorter than the measured ones.

To analyze the stability of the sensor, as shown in Fig. 7, *a*, *b*, 65 % and 95 % are measured for 180 minutes at relative humidity levels where the wavelength and power change linearly. this indicates that the sensor is stable in Fig. 7, *c*, the cross-sensitivity of the sensor was determined by the spectrum of the fiber laser at different temperatures. When the ambient temperature increases from 25 °C to 44 °C, the emission wavelength of the fiber laser sensor changes from 1530.19 nm to 1530.64 nm, and the output power decreases from – 36.64 dBm to – 37.12 dBm. The low temperature cross sensitivity is – 0.025 dB/°C and 0.024 nm/°C. This indicates that the Fabry-Perot interferometer is due to the low thermal expansion of the resonator. Therefore, the calibration of the sensor still needs to be improved.

Compared with other reviews, based on the presented results, it was explained that this sensor has novel design, simple sensor technology, stability and fast response. it can

help to improve the safety and efficiency of new fiber optic sensors for monitoring implantable integrated circuits.

7. Conclusions

1. The study shows that using a combination of a Fabry-Perot interferometer and Fiber Bragg Grating significantly improves the accuracy of temperature and humidity measurements. The results of the study show that the measurement parameters of the sensor enable accurate measurement without affecting each other. By using this method, the efficiency and accuracy of the sensor are significantly increased compared to existing methods, making it effective for use in various applications.

2. During the experimental tests, the variation of the sensor parameters as a function of response time and temperature was studied. The results showed that the response time of the sensor was about 72 ms and the recovery time was about 357 ms. These indicators point to the sensor's ability to respond quickly, making it suitable for real-time monitoring. Over the temperature range of –5 °C to 70 °C, the sensor parameters remained stable.

3. During the study, the influence of external factors, including mechanical vibrations, on the accuracy of the sensor was tested. As a result, the sensor design is resistant to mechanical vibrations, which does not affect its measurement accuracy. The resistance of the sensor to mechanical vibration is an important advantage in long-term applications and makes it suitable for use in industrial environments.

The high sensitivity and accuracy of the sensor results is due to the combination of the Fabry-Perot interferometer and the Fiber Bragg Grating combination. The sensor's measurement parameters for temperature and humidity are designed so that they do not influence each other, which increases its stability. In addition, the sensor's resistance to mechanical vibrations ensures reliable operation in real-world applications. The sensitivity of the sensor in measuring temperature and humidity was higher than existing sensors. The response time of the sensor is 72 ms and recovery time – 357 ms, indicating that it is suitable for real-time monitoring. The resistance of the sensor to mechanical vibration allows the sensor to be used in the long term, which is an important advantage in both industry and academia.

Conflict of interest

The authors declare that they have no conflict of interest in relation to this research, whether financial, personal, authorship or otherwise, that could affect the research and its results presented in this paper.

Financing

This is a result based on an experiment conducted in the optical fiber transmission laboratory, following the direction of our dissertation work.

Data availability

Manuscript has associated data in a data repository.

Use of artificial intelligence

The authors confirm that they did not use artificial intelligence technologies when creating the current work.

References

1. Rao, X., Zhao, L., Xu, L., Wang, Y., Liu, K., Wang, Y. et al. (2021). Review of Optical Humidity Sensors. Sensors, 21 (23), 8049. https://doi.org/10.3390/s21238049
2. Kolpakov, S., Gordon, N., Mou, C., Zhou, K. (2014). Toward a New Generation of Photonic Humidity Sensors. Sensors, 14 (3), 3986–4013. https://doi.org/10.3390/s140303986
3. Fan, L., Bao, Y. (2021). Review of fiber optic sensors for corrosion monitoring in reinforced concrete. Cement and Concrete Composites, 120, 104029. https://doi.org/10.1016/j.cemconcomp.2021.104029
4. Kunelbayev, M., Bigaliyeva, Z., Tuleshov, Y., Ibekeyev, S., Kerimkulov, D. (2023). Thermodynamic Analysis of an Experimental Model of a Solar-Heat Supply System. Processes, 11 (2), 451. https://doi.org/10.3390/pr11020451
5. Hammouche, H., Achour, H., Makhlouf, S., Chaouchi, A., Laghrouche, M. (2021). A comparative study of capacitive humidity sensor based on keratin film, keratin/graphene oxide, and keratin/carbon fibers. Sensors and Actuators A: Physical, 329, 112805. https://doi.org/10.1016/j.sna.2021.112805
6. Schindelholz, E., Risteen, B. E., Kelly, R. G. (2014). Effect of Relative Humidity on Corrosion of Steel under Sea Salt Aerosol Proxies. Journal of The Electrochemical Society, 161 (10), C450–C459. https://doi.org/10.1149/2.0221410jes
7. Huang, C., Xie, W., Yang, M., Dai, J., Zhang, B. (2015). Optical Fiber Fabry–Perot Humidity Sensor Based on Porous Al2O3 Film. IEEE Photonics Technology Letters, 27 (20), 2127–2130. https://doi.org/10.1109/lpt.2015.2454271
8. Mekhtiyev, A., Dunayev, P., Neshina, Y., Alkina, A., Aimagambetova, R., Mukhambetov, G. et al. (2023). Power supply via fiber-optical conductor for sensors of mine working monitoring system. Eastern-European Journal of Enterprise Technologies, 5 (5 (125)), 15–23. https://doi.org/10.15587/1729-4061.2023.289775
9. Abdykadyrov, A., Marxuly, S., Tashtay, Y., Kuttybayeva, A., Sharipova, G., Anar, K. et al. (2023). Study of the process of cleaning water-containing iron solutions using ozone technology. Water Conservation & Management, 7 (2), 148–157. https://doi.org/10.26480/wcm.02.2023.148.157
10. Zhao, C., Yuan, Q., Fang, L., Gan, X., Zhao, J. (2016). High-performance humidity sensor based on a polyvinyl alcohol-coated photonic crystal cavity. Optics Letters, 41 (23), 5515. https://doi.org/10.1364/ol.41.005515

11. Budnicki, D., Parola, I., Szostkiewicz, L., Markiewicz, K., Holdynski, Z., Wojcik, G. et al. (2020). All-Fiber Vector Bending Sensor Based on a Multicore Fiber With Asymmetric Air-Hole Structure. Journal of Lightwave Technology, 38 (23), 6685–6690. https://doi.org/10.1109/jlt.2020.3012769
12. Mathew, J., Semenova, Y., Farrell, G. (2013). Effect of coating thickness on the sensitivity of a humidity sensor based on an Agarose coated photonic crystal fiber interferometer. Optics Express, 21 (5), 6313. https://doi.org/10.1364/oe.21.006313
13. Ekechukwu, G. K., Sharma, J. (2021). Well-scale demonstration of distributed pressure sensing using fiber-optic DAS and DTS. Scientific Reports, 11 (1). https://doi.org/10.1038/s41598-021-91916-7
14. Lu, F., Wright, R., Lu, P., Cvetic, P. C., Ohodnicki, P. R. (2021). Distributed fiber optic pH sensors using sol-gel silica based sensitive materials. Sensors and Actuators B: Chemical, 340, 129853. https://doi.org/10.1016/j.snb.2021.129853
15. Zheng, X., Shi, B., Zhang, C.-C., Sun, Y., Zhang, L., Han, H. (2021). Strain transfer mechanism in surface-bonded distributed fiber-optic sensors subjected to linear strain gradients: Theoretical modeling and experimental validation. Measurement, 179, 109510. https://doi.org/10.1016/j.measurement.2021.109510
16. Mikhailov, P., Ualiyev, Z., Kabdoldina, A., Smailov, N., Khikmetov, A., Malikova, F. (2021). Multifunctional fiber-optic sensors for space infrastructure. Eastern-European Journal of Enterprise Technologies, 5 (5 (113)), 80–89. https://doi.org/10.15587/1729-4061.2021.242995
17. Zhu, C., Zheng, H., Ma, L., Yao, Z., Liu, B., Huang, J., Rao, Y. (2023). Advances in Fiber-Optic Extrinsic Fabry–Perot Interferometric Physical and Mechanical Sensors: A Review. IEEE Sensors Journal, 23 (7), 6406–6426. https://doi.org/10.1109/jsen.2023.3244820
18. Liu, Z., Zhao, B., Zhang, Y., Zhang, Y., Sha, C., Yang, J., Yuan, L. (2022). Optical fiber temperature sensor based on Fabry-Perot interferometer with photopolymer material. Sensors and Actuators A: Physical, 347, 113894. https://doi.org/10.1016/j.sna.2022.113894
19. Barmpakos, D., Kaltsas, G. (2021). A Review on Humidity, Temperature and Strain Printed Sensors – Current Trends and Future Perspectives. Sensors, 21 (3), 739. https://doi.org/10.3390/s21030739
20. Zhao, F., Lin, W., Hu, J., Liu, S., Yu, F., Chen, X. et al. (2022). Salinity and Temperature Dual-Parameter Sensor Based on Fiber Ring Laser with Tapered Side-Hole Fiber Embedded in Sagnac Interferometer. Sensors, 22 (21), 8533. https://doi.org/10.3390/s22218533
21. Ge, Q., Zhu, J., Cui, Y., Zhang, G., Wu, X., Li, S. et al. (2022). Fiber optic temperature sensor utilizing thin PMF based Sagnac loop. Optics Communications, 502, 127417. https://doi.org/10.1016/j.optcom.2021.127417
22. Zhao, F., Xiao, D., Lin, W., Chen, Y., Wang, G., Hu, J. et al. (2022). Sensitivity Enhanced Refractive Index Sensor With In-Line Fiber Mach-Zehnder Interferometer Based on Double-Peanut and Er-Doped Fiber Taper Structure. Journal of Lightwave Technology, 40 (1), 245–251. https://doi.org/10.1109/jlt.2021.3118285
23. Zhao, Y., Zhao, J., Wang, X., Peng, Y., Hu, X. (2022). Femtosecond laser-inscribed fiber-optic sensor for seawater salinity and temperature measurements. Sensors and Actuators B: Chemical, 353, 131134. https://doi.org/10.1016/j.snb.2021.131134
24. Liang, H., Wang, J., Zhang, L., Liu, J., Wang, S. (2022). Review of Optical Fiber Sensors for Temperature, Salinity, and Pressure Sensing and Measurement in Seawater. Sensors, 22 (14), 5363. https://doi.org/10.3390/s22145363
25. Wang, L., Wang, Y. jie, Song, S., Li, F. (2021). Overview of Fibre Optic Sensing Technology in the Field of Physical Ocean Observation. Frontiers in Physics, 9. https://doi.org/10.3389/fphy.2021.745487
26. Yu, Y., Bian, Q., Lu, Y., Zhang, X., Yang, J., Liang, L. (2019). High Sensitivity All Optical Fiber Conductivity-Temperature-Depth (CTD) Sensing Based on an Optical Microfiber Coupler (OMC). Journal of Lightwave Technology, 37 (11), 2739–2747. https://doi.org/10.1109/jlt.2018.2878475
27. Akter, S., Ahmed, K., El-Naggar, S. A., Taya, S. A., Nguyen, T. K., Dhasarathan, V. (2020). Highly Sensitive Refractive Index Sensor for Temperature and Salinity Measurement of Seawater. Optik, 216, 164901. https://doi.org/10.1016/j.ijleo.2020.164901
28. Li, H., Qian, X., Zheng, W., Lu, Y., E, S., Zhang, Y. (2020). Theoretical and experimental characterization of a salinity and temperature sensor employing optical fiber surface plasmon resonance (SPR). Instrumentation Science & Technology, 48 (6), 601–615. https://doi.org/10.1080/10739149.2020.1762204
29. Ramakrishnan, M., Rajan, G., Semenova, Y., Farrell, G. (2016). Overview of Fiber Optic Sensor Technologies for Strain/Temperature Sensing Applications in Composite Materials. Sensors, 16 (1), 99. https://doi.org/10.3390/s16010099
30. Zhou, J., Guo, J., Chang, M., Chen, Z., Zhao, D., Jia, B. (2022). Moisture sensitive composite fiber based on agarose gel surface modification. Microwave and Optical Technology Letters, 64 (12), 2289–2293. https://doi.org/10.1002/mop.33429
31. Grogan, C., McGovern, F. R., Staines, R., Amarandei, G., Naydenova, I. (2021). Cantilever-Based Sensor Utilizing a Diffractive Optical Element with High Sensitivity to Relative Humidity. Sensors, 21 (5), 1673. https://doi.org/10.3390/s21051673
32. Zhang, B.-K., Tan, C.-H. (2017). A Simple Relative Humidity Sensor Employing Optical Fiber Coated with Lithium Chloride. Physical Science International Journal, 16 (4), 1–6. https://doi.org/10.9734/psij/2017/37309
33. He, C., Korposh, S., Correia, R., Liu, L., Hayes-Gill, B. R., Morgan, S. P. (2021). Optical fibre sensor for simultaneous temperature and relative humidity measurement: Towards absolute humidity evaluation. Sensors and Actuators B: Chemical, 344, 130154. https://doi.org/10.1016/j.snb.2021.130154
34. Zhang, J., Xie, Y., Zhang, Z., Lv, L., Tan, Z. (2021). Research on Optical Fiber Sensor for Environmental Temperature and Humidity of Transmission Line. E3S Web of Conferences, 252, 02014. https://doi.org/10.1051/e3sconf/202125202014
35. Wen, H.-Y., Liu, Y.-C., Chiang, C.-C. (2020). The use of doped conductive bionic muscle nanofibers in a tennis racket–shaped optical fiber humidity sensor. Sensors and Actuators B: Chemical, 320, 128340. https://doi.org/10.1016/j.snb.2020.128340